On the Effects of Non-ideal Signal Sources in Automotive Short Range FM-CW Sensors

Winfried Mayer, Wolfgang Menzel

University of Ulm, Microwave Techniques, Albert-Einstein-Allee 41, 89081 Ulm, Germany,
Phone ++49 731 50 26360, Fax ++49 731 50 26359, winfried.mayer@ieee.org

***Abstract*— Investigations on the effects of non-ideal signal sources on system performance of short and medium range automotive FM-CW radar sensors are presented. The investigations have been carried out with a specially created simulation model. The model allows the simulation of the time domain IF signal of a homodyne radar scan with multiple targets taking into account spectral noise, sweep nonlinearities of a synthesized signal source, and LO leakage. After a short discussion of the special problems in FM-CW radars for short and medium range automotive sensors, an overview is given on the model's theory and implementation. To verify the simulation model, exemplary results are compared with data measured by an experimental sensor setup. The model is then applied to the particular problem of finding the optimum control bandwidth for the synthesized signal source of a 24 GHz FM-CW sensor.**

I. Introduction

Driven by the demands of the automotive industry, various short and medium range radar sensor concepts have been explored in the last years. Their common requirement is to detect and localize obstacles in a lane in front of the vehicle [1], [2]. The observing area should be resolved in two dimensions, usually range and cross range by electronic means. The typical traffic sceneries that fall into the required observing area can contain many scattering objects with very different radar cross sections. Moreover, some of the objects have radar cross sections that vary with distance as for example vertical posts and walls. To be able to detect and localize objects with relatively small radar cross sections particularly pedestrians close to strongly reflecting cars a high target dynamic range is desirable. In addition to the mentioned functional requirements, automotive sensors have to be low cost and small size, limiting choices and performance of RF building blocks.

II. Limitations in short range FM-CW sensors caused by imperfect signal sources

The target dynamic range of homodyne FM-CW sensors in a specific range gate is generally limited by the spectral noise and modulation side bands of strong adjacent targets including the always present quasi zero-range-target caused by the local oscillator (LO) leakage. Improvements of spectral purity can reduce the magnitudes and widths of the sidebands and therefore rise the target dynamic range. In a coherent FM-CW sensor with a synthesized signal source as depicted in Fig. 1, there is some margin to influence spectral noise by the choice of the PLL control bandwidth and its natural frequency, respectively. However, with low control bandwidths, the PLL can not follow fast frequency ramps anymore, causing distortions of sweep linearity. These distortions are modulating the intermediate frequency (IF) output signal in frequency and therefore smearing the target response. On the other hand, very high control bandwidths are often limited by component parameters and can cause spurious signal problems.

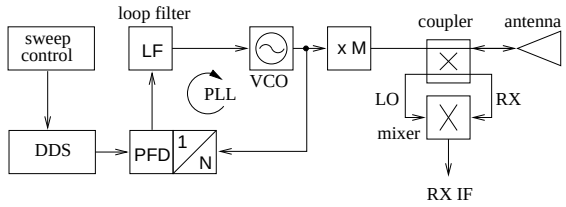

Fig. 1. Simplified block diagram of the signal generation in a 24 GHz radar sensor.

To check whether the design of a signal source is practical in a short range scenery, numerical simulations covering its major non-ideal effects, would be very helpful. From this need, various behavior models have been composed and compiled to a Simulink[1] FM-CW model. As for a first practical application, the FM-CW model is applied to finding the optimum control bandwidth for the PLL in the structure in Fig. 1 for a near range scenery from 0 to 50 m.

III. Description of the simulation model

With the Simulink model, the time domain IF signal of a homodyne radar scan from multiple targets taking into account colored amplitude and phase noise, AM and PM spurs and sweep linearity distortions caused by the PLL can be simulated. The amplitude and phase envelopes of the IF signals for multiple targets are calculated for fixed time steps kt_s from various input parameters describing deterministic and stochastic attributes of the building blocks. Fig. 2 shows the simplified block diagram of the kernel of the simulation model. In the ideal (noise- and

[1]® The MathWorks, Inc.

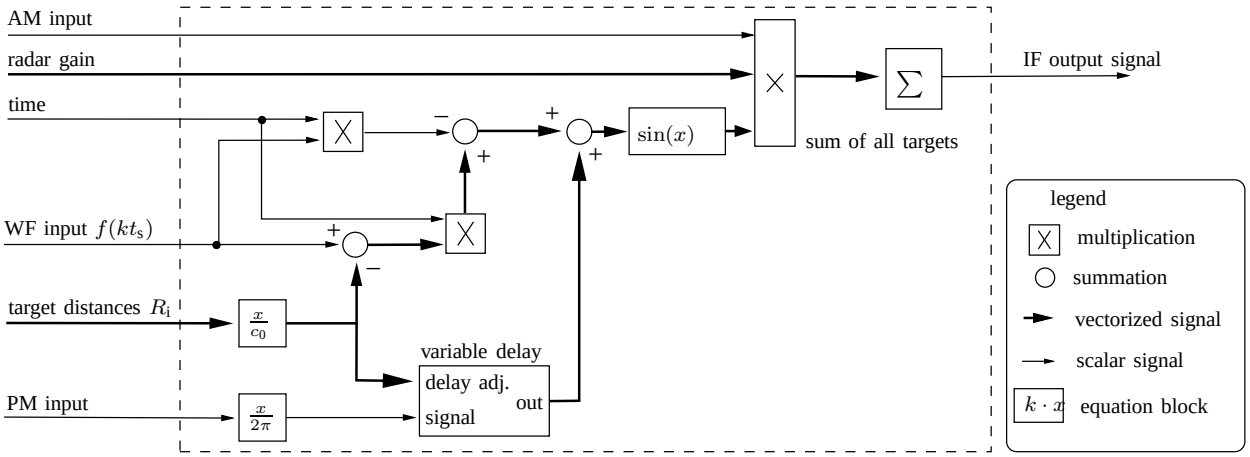

Fig. 2. Kernel of the FM-CW model.

distortion-free) case the IF output signal of the model for a number of targets with distances R_i and for an input frequency ramp $f(kt_\mathrm{s}) = f_0 + S \cdot kt_\mathrm{s}$ is,

$$u_\mathrm{IF}(kt_\mathrm{s}) = -\sum_i G_\mathrm{i} \cdot \sin\left(2\pi f_0 \tau_\mathrm{i} + 2\pi S k t_\mathrm{s} \tau_\mathrm{i}\right) \qquad (1)$$

with $\tau_\mathrm{i} = 2 \cdot R_\mathrm{i}/c_0$ the target delays and G_i the radar gains. G_i are depending on the targets' ranges, radar cross sections and the sensor parameters contributing to a simple radar equation. The model implies that the integration to get the instantaneous phase from the instantaneous frequency $\phi(t) = \int_0^t f(\tau)d\tau$ can be approximated by $\phi(t) \approx t \cdot f(t)$. Without the necessity to know the absolute phases of the targets and for moderate sweep nonlinearities this approximation is very practical. It avoids numerical integration of $f(kt_\mathrm{s})$ and therefore simplifies the model's kernel. For simulation of spectral noise and spurious signals, the phase and the amplitude of the IF signal can be modulated via the inputs AM and PM in Fig. 2. In the case of PM modulation the compression factor describing the correlation of the phase noise in a homodyne FM-CW architecture is taken into account by using a variable transport delay block available in Simulink. As this block has to interpolate or even extrapolate [3] for delays τ_i in the range of the simulation time steps, it is becoming imprecise for very close targets. For that the variable delay element is not used for the simulation kernel. However, to delay the phase noise signals it has been found accurate enough. The local oscillator leakage effects are modeled by adding a short range target to the simulated targets. The radar cross section of this additional target is derived from the input LO-leakage value and its range can be estimated from the RF layout. The limitations of the variable delay line elements increase the compression factor and therefore can lead to an overestimation of the LO-effects in the simulation.

To be able to plug the model into higher level simulations, the simulation times are kept short by the avoidance of recursive blocks. The simulation sampling rate $1/t_\mathrm{s}$ is chosen by a factor of 30 to 100 higher than the real system's sampling times to be able to simulate the effects of analog IF processing stages and to improve accuracy of the PM compression factor. Simulating one radar scan with 16K samples on a normal PC takes less than one second.

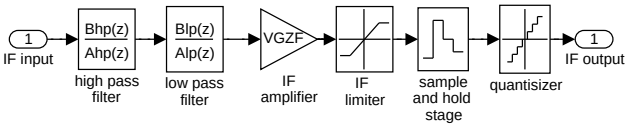

Fig. 3. Simulink model of the IF stage.

As in a real system, the IF output signals of the simulation kernel are processed by an IF stage. In that IF stage a number of standard Simulink blocks are used to model the analog baseband processing and the analog to digital conversion. Fig. 3 shows the Simulink block diagram of the currently implemented IF stage 3. It includes two filters to confine the IF frequency range, an IF amplifier and the three blocks limiter, sample and hold, and quatisizer forming together a simple analog-to-digital converter.

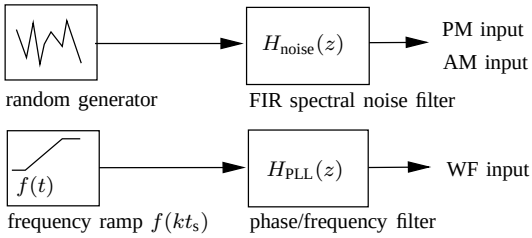

Fig. 4. Principles to model the non-ideal signal source.

A. Simulation of spectral noise

To simulate spectral noise, the outputs of random number generators are valued by finite impulse response

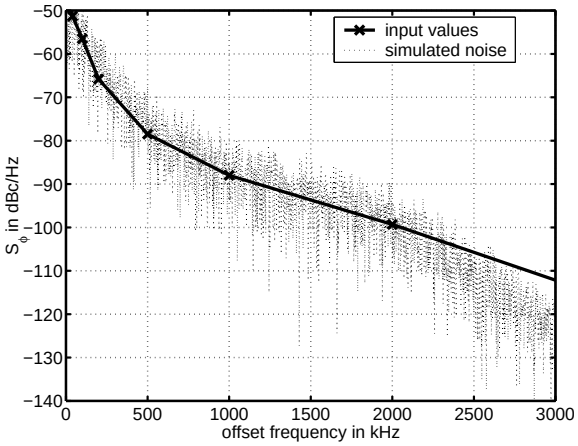

Fig. 5. Exemplary simulation of PM noise S_ϕ. The x-marked curve describes the input values for the calculation of the filter coefficients, the dotted curve the power spectral density of a simulated noise sequence of 16384 samples with sampling time $t_\mathrm{s} = 52\,\mathrm{ns}$. The order of the used FIR filter is 400.

(FIR) digital filters. The coefficients of the filters are derived from input data describing the source's AM and PM noise. The amplitude of the random generators is normalized to the Nyquist bandwidth of the sampling rate in the simulation. For calculation of the filter coefficients, the frequency sampling method is used [4], [5]. In this method time domain samples obtained from the inverse Fourier transform of samples of the desired frequency response are taken as coefficients for the FIR filter. To avoid side-lobes in the stop bands caused by the finite length of the impulse response a Kaiser window is applied to the filter coefficients. The derivation of the filter coefficients requires linearly spaced frequency samples starting from frequency 0 to half of the sampling frequency $f_\mathrm{s} = 1/t_\mathrm{s}$ of the simulation. If the time step t_s of the simulation is chosen very short, e.g. to reduce overestimation of the LO-leakage effects, it must be ensured that the filter order is high enough to describe the low frequency components of the noise to be simulated.

Though not being very efficient in the number of coefficients required to approximate a desired frequency response, the method has the advantage of modeling arbitrary noise shapes with acceptably good accuracy. The input noise shapes can be obtained from phase noise measurements or circuit simulations. The approximation errors are low, if there are no steep transitions and slopes in the filter response. This is normally the case for phase and amplitude noise envelopes, so the method is well suited to this problem. In Fig. 5 the simulation of a PM noise envelope is demonstrated. In comparison to the methods presented in [6] and [7], the here presented approach with FIR filters is more flexible, because it allows to simulate any colored noise in time domain based on available frequency domain data.

By feeding harmonic signals into the PM- or the AM-port of the simulation kernel, the effects of spurious signals can be analyzed, too.

B. Simulation of modulation non-linearities caused by a PLL

In the signal generation architecture depicted in Fig. 1 a PLL is used to transfer the frequency modulation waveform generated by the DDS from the baseband to the desired RF frequency band. In this transformation the limited bandwidth of the PLL is deforming the waveform. The limited bandwidth of the PLL is modeled by filtering the input waveform $f(kt_\mathrm{s})$ by a digital low pass filter (see Fig. 4). The filter is representing the forward phase transfer function of the PLL and its coefficients are obtained from the PLL synthesis. With system theory it can be shown that it is equivalent to filter the frequency or the phase waveform, if absolute phase terms can be omitted. In a typical FM-CW radar the frequency deviation is several orders of magnitude higher than the IF frequency caused by a target, so even very small changes in the modulation waveform produce considerable errors in the IF signal. For that reason the passband of the PLL representing filter must be modeled very accurate, which is not possible with the general FIR approach used to model noise. If PLL design data are not available, maximally flat low pass filters, e.g. of Butterworth type, having a corner frequency equal to the PLL's natural frequency, is found to be practical to approximate the forward transfer function. A third order PLL needs to be modeled by a second order butterworth low pass with 40 dB/decade slope in the stop band upside the natural frequency of the loop. This results in a 3rd order digital filter design.

IV. Experimental verification of the model

Although the simulation model is designed to optimize the imaging radar sensor presented in [8], a simple one channel monostatic sensor setup composed of a level sensor module [9], a separate PLL board, a horn antenna, and a DDS module is used for verification of the simulations. The setup realizes the architecture of Fig. 1 with a high degree of flexibility and a bandwidth of up to 2 GHz, which is helpful in masking out the examined effects from other influences. In addition an idealized target scenery with one strong reflecting target is necessary so that the examined signal source effects are not hidden by clutter reflections.

In a first setup a 40 cm corner reflector with appr. $190\,\mathrm{m}^2$ radar cross section is measured in an absorbing chamber. Due to the limited size of the anechoic chamber, the reflector is only at a distance of $R = 5.3\,\mathrm{m}$. The simulation parameters are set to the parameters of the sensor setup and the scenery. A summary of these parameters is given in Table I.

Some test results are depicted in Fig. 6. All radar responses are calculated from the IF time domain signals by a fast Fourier transformation with zero padding for higher range accuracy and a time domain window function for 60 dB side lobe suppression. Exactly the same processing

Parameter	value
center frequency	24.5 GHz
frequency deviation	1 GHz
transmit power	8 dBm
over all conversion gain	20 dB
antenna gain	19 dB
waveform	up-ramp
sweep time	950 µs
PLL bandwidth	40 kHz
IF bandwidth	10 kHz–250 kHz
sampling rate	600 kHz
ADC	12bit
# samples recorded	256
phase noise	see Fig. 5
target radar cross section	189m^2
target distance	5.3 m

TABLE I

PARAMETERS OF THE SENSOR SETUP AND THE RADAR SCENERY FOR THE VERIFICATION MEASUREMENTS.

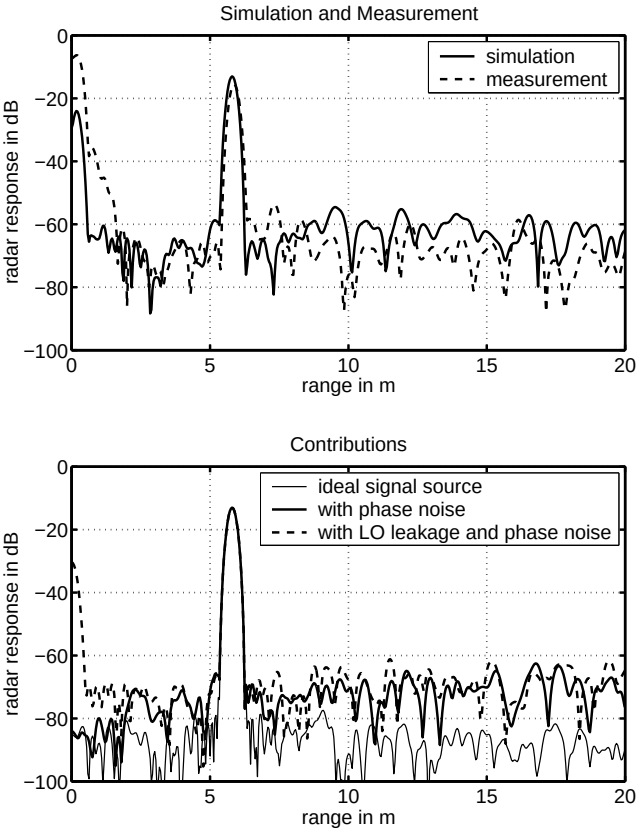

Fig. 6. Diagrams on the verification of the simulation model.

is applied to the time domain data from measurements and from simulations. In the top diagram the simulation results including the effects of phase noise, local oscillator leakage, and modulation nonlinearity of the used PLL design are compared with the test measurements. Simulation and measurement show good agreement in the target dynamic range, which is in the range of 40 dB and in the target's shape. However there are discrepancies in the simulated and measured zero range target caused by LO leakage. Despite a worst case assumption of only 12 dB LO suppression, the measured zero range target is much higher than predicted by the simulation. In the bottom diagram of Fig. 6 the simulated target responses with an ideal signal source are plotted together with the simulated target responses taking into account phase noise only and LO-leakage plus phase noise. From this comparison, it can be deduced, that the largest contribution to the noise floor is the phase noise modulating the target signal. The second largest contribution is the zero range target caused by LO-leakage with its noise side-bands. The margin for modifications in the available radar setups and limitations in creating idealized target sceneries, have prevented experimental verification of the simulated PLL sweep non-linearities.

V. OPTIMIZATION OF A SIGNAL SOURCE

The FM-CW simulation model is combined with the formulas for PLL loop-filter synthesis and an available PLL phase noise simulation library, in which the theory of [10] has been implemented. With this combination the synthesized signal of the given FM-CW sensor architecture is analyzed and optimized for ranges from 0–50 m. The results of a series of simulations, using realistic PLL parameters deduced from measured data of the available experimental sensors, can be summarized in the following statements: the PLL sweep nonlinerities are significantly influencing the target responses only if the product of sweep time and natural frequency $T_\text{s} \cdot f_\text{n,PLL}$ is becoming smaller than 5. The best value for the natural frequency is the one that minimizes the integral of phase noise within the sensor's IF bandwidth. With high phase noise contributions from the VCO but low noise contributions from the other synthesizer blocks and for short sweep times, the optimum is the highest possible natural frequency. If the VCO phase noise contributions are low and the sweep times are short, the optimum will be found at low natural frequencies. The highest possible natural frequency is limited in practice by feasibility of the loop-filter components. Additionally, the VCO phase noise performance often decreases for high natural frequencies because of the low capacitive load at the tuning input.

In Fig. 7 the simulated target responses for 8 targets and the associated phase noise envelopes are plotted for two much differing natural frequencies (20 kHz and 1 MHz)for an exemplary sensor similar to the one in [8]. The sensor parameters are given in the figure's caption.

VI. CONCLUSION

The effects of non-ideal signal sources in short range FM-CW sensors have been discussed, and a model for the simulation of spectral noise, modulation nonlinearities, and local oscillator leakage has been presented in detail. The simulation model has been verified qualitatively with a simple sensor setup. Finally, the simulation model was applied to optimize the signal source for an exemplary

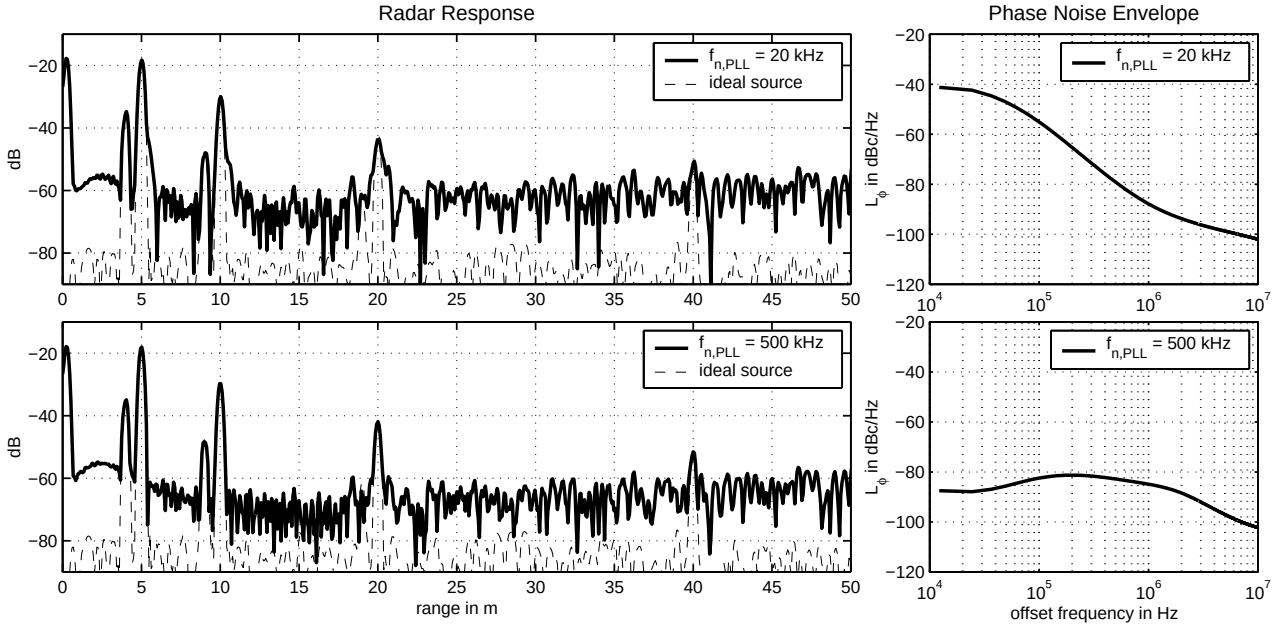

Fig. 7. Simulated spectra of 8 targets with alternating radar cross sections of $1m^2$ and $100m^2$ at distances of 4, 5, 9, 10, 19, 20, 39, and 40 m for two different PLL control bandwidths 20 kHz (top) and 1000 kHz (bottom). In the right hand diagrams the single side band phase noise envelopes L_ϕ of the corresponding PLL designs are plotted. Limited control bandwidth of the PLL causes deformations in the target responses in the top diagram. Further parameters but still not an exhaustive list are: Frequency deviation: 1 GHz, sweep time: 330 µs, sampling rate: 6.25 MHz, 2048 samples, transmit power: 8 dBm, conversion gain: 30 dB, antenna gains RX and TX: 12 dB, IF bandwidth: 8 kHz– 3.125 MHz, ADC: 12bit, LO-leakage: -12 dB at an electrical length of 0.5 m, phase noise of the VCO: similar to Fig. 5

medium range FM-CW radar sensor. In the near future, the FM-CW model will be used to analyze the influences of non-ideal signal sources on the two dimensional radar responses of the imaging sensor presented in [8].

VII. Acknoledgement

The authors would like to acknowledge the support by component samples and test equipment from the Microwave Factory at EADS in Ulm, Germany.

References

[1] R. Schneider and J. Wenger, "System aspects for future automotive radar," in *IMS, Digest*, 1999, pp. 293–296.

[2] R. Mende and H. Rohling, "New automotive applications for smart radar systems," in *German Radar Symposium (GRS) Proceedings*. DGON, September 2002, pp. 35–40.

[3] MathWorks, Ed., *Simulink, Dynamic System Simulation for Matlab, Using Simulink*, vers. 3 ed. The MathWorks Inc., 1999.

[4] S. A. Azizi, Ed., *Entwurf und Realisierung digitaler Filter*, 5th ed. Oldenburg, 1990, ch. 6.2.2 Frequenzabtastung, pp. 256–263.

[5] MathWorks, Ed., *Signal processing toolbox for use with matlab, user's guide*, vers.4.2 ed. The MathWorks Inc., 1999.

[6] J. J. M. de Wit and P. Hoogeboom, "High resolution FM-CW SAR performance analysis," in *Geoscience and Remote Sensing Symposium, 2003. IGARSS '03. Proceedings. 2003 IEEE International*, vol. 7, July 2003, pp. a4317–a4319.

[7] M. E. Adammski, K. S. Kulpa, M. Nalecz, and A. Wojtkiewicz, "Phase noise in two-dimensional spectrum of video signal in FMCW homodyne radar," in *Radar and Wireless Communications. 2000. MIKON-2000. 13th International Conference on*, vol. 2, May 2000, pp. 645 – 648.

[8] W. Mayer, S. Buntz, H. Leier, and W. Menzel, "Imaging radar sensor front-end with a large transmit array," in *European Radar Conference (EuRad), Conference Proceedings*, vol. 3, no. 9, 2004, pp. 153–156.

[9] J. A. Kielb and M. O. Pulkrabek, "Application of a 25 GHz FMCW radar for industrial control and process level measurement," in *IEEE MTT-S Int. Microwave Symposium (IMS) Digest*, vol. I, 1999, pp. 281–284.

[10] V. F. Kroupa, "Noise properties of PLL systems," *IEEECOM*, vol. 30, no. 10, pp. 2244–2252, October 1982.